Geometry and electronic structures of magic transition-metal oxide clusters M_9O_6 (M=Fe, Co, and Ni)

Q. Sun, M. Sakurai, Q. Wang, and J. Z. Yu
Institute for Materials Research, Tohoku University, Sendai 980-77, Japan

G. H. Wang
Department of Physics and National Laboratory of Solid State Microstructures, Nanjing University, Nanjing 210093, People's Republic of China

K. Sumiyama and Y. Kawazoe
Institute for Materials Research, Tohoku University, Sendai 980-77, Japan

(Received 23 December 1999; revised manuscript received 1 May 2000)

The magic oxide clusters M_9O_6 (M=Fe, Co, Ni) are found by using reactive laser vaporized cluster source. From the first-principles calculations, the possible equilibrium geometries for these three oxide clusters are determined to be a C_{2v} symmetry, where the skeleton composed of 9 metal atoms also has C_{2v} symmetry, different from the equilibrium structures of pure transition metal cluster M_9. The O atoms are energetically more favorable to cap the triangle surfaces. In Fe_9O_6 and Co_9O_6 clusters, oxygen atoms are antiferromagnetically polarized while ferromagnetically polarized in the Ni_9O_6 cluster, similar to the case of O atoms adsorbed on the reconstructed Ni(110) surface. The magnetic behaviors are explained from electronic structures.

I. INTRODUCTION

The discovery of magic numbers in CsI (Ref. 1) and Xe clusters (Ref. 2) started a new era in cluster science. Since then, many scientists over the world have been studying about clusters and already made great progress.[3] In recent years, together with the development of new experimental techniques and a more exact *ab initio* calculation method, oxide clusters have become a new field of research due to the following reasons: first, from the practical point of view, oxygen contamination can occur during the preparation of clusters; second, oxide clusters can be used as models for oxide surfaces; third, oxidation can be used as a new way to modulate the structure and property of clusters. As a matter of fact, many studies have been devoted to the oxidation of simple metal clusters: Li_n,[4–6] Na_n,[7,8] Cs_n,[9–11] Ca_n,[12–14] Mg_n,[12,13,15,16] Ba_n,[14,17] Al_n,[18–20] and Sb_n clusters.[21]

For the transition-metal oxide clusters, however, only two systems have mainly been studied: Fe_nO_m (Refs. 22–26) and Mn_nO_m (Refs. 27–32) clusters. Small iron oxide clusters are extensively studied by Wang and co-workers,[22–24] the photoelectron spectra for $Fe_mO_n^-$ ($m=1-4$, $n=1-6$) indicated that there exist sequential oxygen atom chemisorptions on surfaces of small iron clusters that provide novel model systems to understand the electronic structure of bulk iron oxides.[22] The equilibrium geometry and electronic structures of the magic $Fe_{13}O_8$ cluster were studied in our previous work.[25–27] As for the Mn-O system, the *ab initio* calculations have been performed for small stoichiometric $(MnO)_n$ clusters ($n \leqslant 9$).[28] Due to the observation of resonant quantum tunneling of spin in single-crystal $Mn_{12}O_{12}$ acetate, the $Mn_{12}O_{12}$ cluster also attracts great attention.[29–33] However, compared with Fe and Mn oxide clusters, the research on Co and Ni oxide clusters is far from complete. Freas and colleagues[34] prepared Co oxide clusters with sputtering and found that the stoichiometric clusters are abundant, and the possible structures were studied with classical pair-potential model in their study. For Ni, only the nickel monoxide molecule[35–37] (NiO) and the nickel dioxide molecule[35] (NiO_2) have been studied.

Recently, we produced Fe, Co, and Ni oxide clusters by using a reactive laser vaporized cluster source, where a pulsed second harmonic of a Nd:YAG laser (YAG) denotes yttrium aluminum garnet was used for vaporization of an Fe (Co, Ni) rod. Metal vapor was cooled by He gas injected from a pulsed gas valve synchronizing with a vaporization laser, and oxygen gas was continuously introduced through a small orifice into a cluster formation cell with $10^3\,mm^3$ in volume, with oxygen gas flow rates of 2.3, 0.5, and 2.4 standard cubic centimeters per minute (SCCM) for Fe, Co, and Ni, respectively. The details of the experiment can be found in previous papers.[26,38,39] Figure 1 shows the mass spectra of the clusters. In Ni case, the peaks labeled as *a*, *b*, *c*, *d*, *e*, *f*, *g*, and *h* correspond to Ni_6O_4, Ni_7O_5, Ni_8O_6, $Ni_{10}O_7$, $Ni_{11}O_7$, $Ni_{12}O_8$, $Ni_{14}O_9$, and $Ni_{15}O_9$, respectively. We can see that the intensities in mass spectra for M_9O_6 and $M_{13}O_8$ (M=Fe, Co, and Ni) are much higher than their neighboring peaks, suggesting M_9O_6 and $M_{13}O_8$ are magic clusters. In our experiment, only suboxide clusters are observed, different from the stoichiometric Co oxide clusters found in Ref. 34. One possible reason for this may be due to the different experimental methods and conditions.

As for $M_{13}O_8$, the research on the $Fe_{13}O_8$ cluster has been published before,[25] whereas $Co_{13}O_8$ and $Ni_{13}O_8$ clusters are found to have a structure similar to the $Fe_{13}O_8$ cluster, which will be presented elsewhere.[40] Therefore, the purpose of this

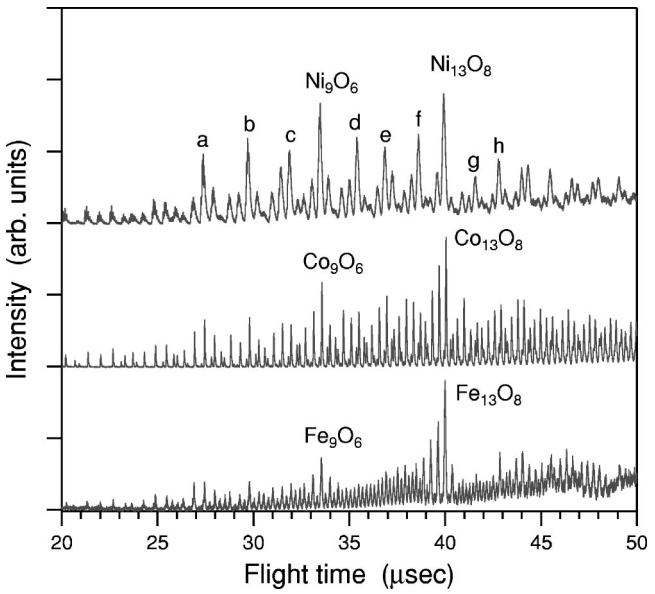

FIG. 1. Time-of-flight mass spectra of positively ionized clusters produced by a reactive vaporization cluster source.

paper is to study M_9O_6 clusters. What are the possible equilibrium geometries? How are the structures changed after oxidation? What are the electronic structures and magnetic properties?

II. COMPUTATIONAL METHOD

A widely used theoretical method for determining the structure is the *ab initio* calculation,[41,42] with which significant progress has been made for simple clusters involving alkali and coinage metals and semiconductors.[43,44] However, for the transition-metal cluster, the open *d* shells give rise to strong electron correlation effects and due to the directional bonding features of *d* orbitals, complicated interactions exist. Furthermore, the number of electrons in the transition-metal cluster increases rapidly with cluster size, all these factors post difficulties in theoretical calculations. In this aspect, the plane-wave basis and ultrasoft pseudopotential method combined with density-functional theory has provided a simple framework,[41,42,45,46] in which the calculation of forces is greatly simplified so that extensive geometry optimization is possible.

In this paper, we used a powerful *ab initio* ultrasoft pseudopotential scheme with a plane-wave basis [Vienna *ab initio* simulation program (VASP)].[47,48] The details can be found in our previous paper.[25] In the optimization, the cluster is placed in a cubic cell with edge length of 12.5 Å, which is sufficiently large to make dispersion effects negligible. In such a big supercell only the Γ point can be used to represent the Brillouin zone. 400 eV has been used as the cutoff energy in the plane-wave expansion of the pseudo-wavefunctions, which is large enough to obtain a good convergence. The structure optimization is symmetry unrestricted, and the optimization is terminated when all the forces acting on the atoms are less than 0.03 eV/Å. In order to obtain more detailed information on the electronic and magnetic properties, molecular orbital calculations[49,50] are performed with the optimized structure. The $3d$, $4s$, and $4p$ orbitals for Fe, Co, and Ni atoms and $2s$ and $2p$ orbitals for the O atom are used as the basis sets.

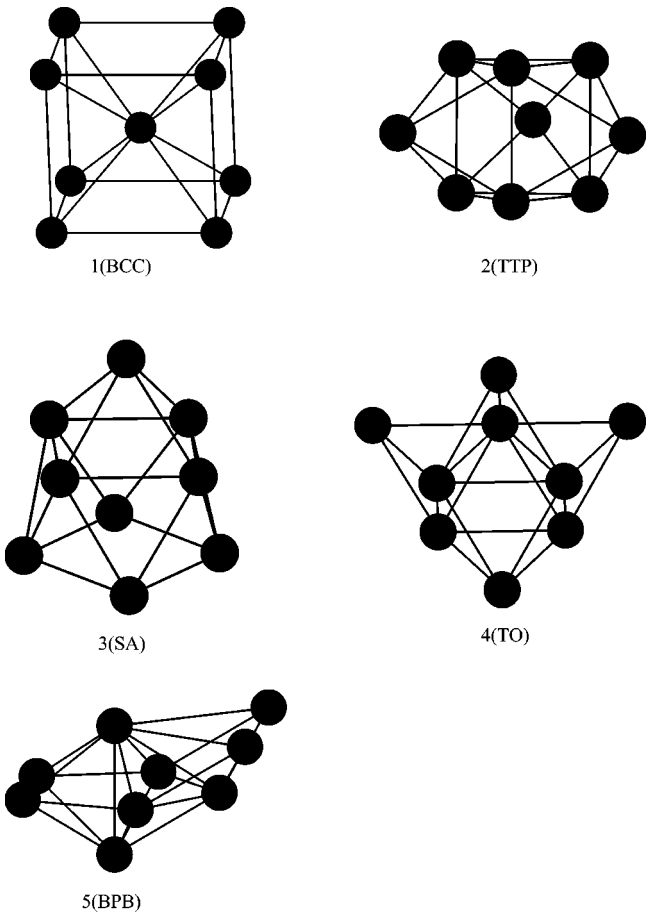

FIG. 2. Five possible structure isomers for the M_9 cluster: body centered cubic (bcc, O_h symmetry), tricapped trigonal prism (TTP, D_{3h} symmetry), square antiprism (SA, C_{4v} symmetry), tricapped octahedron (TO, C_{3v} symmetry), and bicapped pentagonal bipyramid (BPB, C_s symmetry).

III. RESULTS AND DISCUSSIONS

It has been found that the structure of the Fe_9 cluster is body-centered cubic (bcc) with one atom in the center and the other 8 atoms on the surface.[51,52] For the Ni_9 cluster, the corrected effective medium (CEM) theory[53] predicted a tricapped trigonal prism (TTP) structure, while the calculation with the Gupta potential and Finnis-Sinclair potential produced a tricapped octahedron (TO) structure[54] and bicapped pentagonal bipyramid (BPB) structure,[55] respectively. For

TABLE I. Total binding energies (eV) and the final symmetry for M_9O_6 (M = Fe, Co, and Ni) clusters; the corresponding initial structures for pure metal clusters are shown in Fig. 2.

	Symmetry	Fe_9O_6	Co_9O_6	Ni_9O_6
Isomer 1	O_h	−70.089	−69.932	−70.185
Isomer 2	C_{2v}	−82.331	−82.072	−80.060
Isomer 3	C_{2v}	−82.331	−82.072	−80.060
Isomer 4	C_s	−79.836	−72.428	−71.670
Isomer 5	C_s	−80.737	−80.248	−77.940

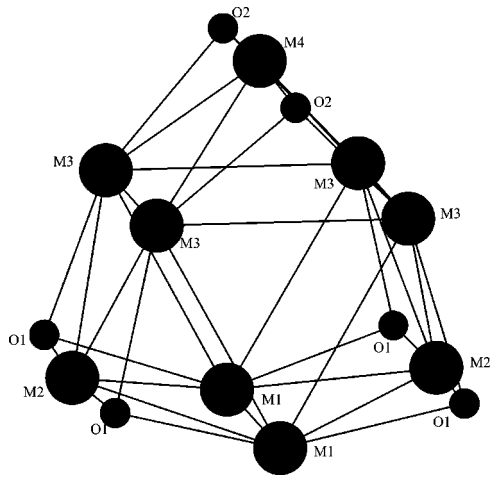

FIG. 3. Optimized structure of M_9O_6 with C_{2v} symmetry.

the Co_9 cluster, a recent experiment[56] suggests possible TTP and TO structures. Besides the structure isomers mentioned above, for the 9-atom cluster, another isomer is the square antiprism (SA) with one atom capped on one square. Figure 2 shows the five structure isomers, from which we search for the possible stable structure for oxide clusters.

In the bcc structure, there are six fourfold adsorption sites that are the possible adsorption positions for six oxygen atoms. For the other structure isomers, according to the previous studies,[22,25] the oxygen atoms are preferably adsorbed nonadjacently on triangle surfaces. TTP, BPB, and TO structures have 14 triangle faces, while the SA structure has 12 triangle faces and one square face. In the initial configurations, the six oxygen atoms are capped nonadjacently on triangle surfaces as symmetrically as possible.

The total binding energies and the final symmetries for the five isomers of oxide clusters are listed in Table I and the corresponding initial structures for the pure metal clusters are shown in Fig. 2. For isomer 1, the initial structure of a pure metal cluster is bcc with O_h symmetry, the final structure of oxide cluster still has O_h symmetry. For isomers 2 and 3, the initial structures of pure metal clusters are TTP and SA with D_{3h} and C_{4v} symmetry, respectively, the final structures of oxide clusters converge to the same symmetry (C_{2v}) with the same energy. In fact, for the pure transition-metal cluster, it has been found that SA structure is quite easily changed into the TTP structure.[57] This is the reason why these two oxide cluster isomers can converge to the same structure. For isomers 4 and 5, their initial structures for pure metal clusters are TO and BPB with C_{3v} and C_s symmetry, respectively, and the final structures of oxide clusters have C_s symmetry with different energy. We can see that the C_{2v} structure produced from isomers 2 and 3 is the most stable among the isomers considered.

In the C_{2v} structure, there are four nonequivalent transition-metal atoms and two nonequivalent oxygen atoms, labeled as $M1$, $M2$, $M3$, $M4$, O1, and O2, respectively, as

TABLE II. Bond length (in Å) and bond angles (in degrees) for M_9O_6 clusters with C_{2v} symmetry.

	Fe_9O_6	Co_9O_6	Ni_9O_6
$r(M1\text{-}M2)$	2.300	2.325	2.418
$r(M1\text{-}M3)$	2.332	2.294	2.383
$r(M2\text{-}M3)$	2.306	2.337	2.415
$r(M3\text{-}M4)$	2.294	2.317	2.414
$r(M1\text{-O1})$	1.871	1.851	1.796
$r(M2\text{-O1})$	1.770	1.755	1.769
$r(M3\text{-O1})$	1.872	1.862	1.798
$r(M3\text{-O2})$	1.871	1.852	1.789
$r(M4\text{-O2})$	1.770	1.772	1.766
α_1	145.2	140.1	156.0
α_2	172.3	160.7	176.5
α_3	145.0	139.9	155.5
α_4	173.5	161.7	178.0

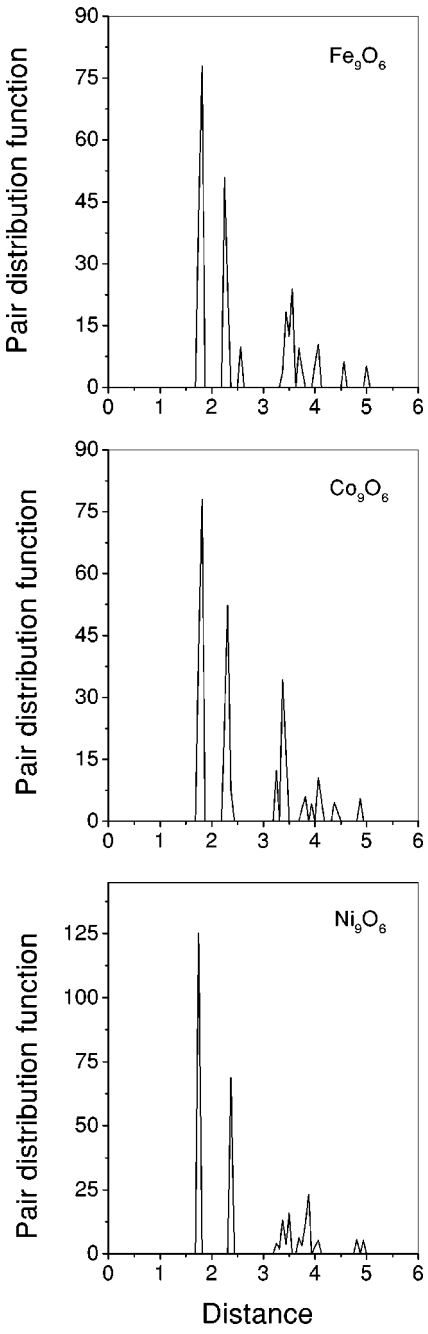

FIG. 4. Pair distribution functions for M_9O_6 clusters with C_{2v} symmetry.

TABLE III. Electronic structures for M_9O_6 clusters with C_{2v} symmetry (energy in eV).

		HOMO					LUMO		
Cluster	E_b	Spin	Energy	Symbol	Electron	Config.	Energy	Symbol	Spin
Fe_9O_6	−82.331	+	−10.993	a_g	1	closed	−10.953	a_g	−
Co_9O_6	−82.072	−	−10.381	a_g	1	closed	−10.370	a_g	−
Ni_9O_6	−80.060	−	−9.316	a_g	1	closed	−9.305	a_g	−

TABLE IV. Main orbital components (%) of HOMO and LUMO for M_9O_6 clusters with C_{2v} symmetry.

	HOMO			LUMO	
Cluster	O $2p$	M $4s$	M $3d$	O $2p$	M $3d$
Fe_9O_6	17.0	21.0	56.0	16.5	78.9
Co_9O_6	7.0	6.1	80.0	9.2	89.2
Ni_9O_6	13.0	13.8	68.0	41.6	53.4

TABLE V. Spin gaps for three oxide clusters with C_{2v} symmetry: $\Delta_1 = -(\epsilon^{+}_{\mathrm{HOMO}} - \epsilon^{-}_{\mathrm{LUMO}})$ and $\Delta_2 - (\epsilon^{-}_{\mathrm{HOMO}} - \epsilon^{+}_{\mathrm{LUMO}})$ (+, spin up; −, spin down).

	$\epsilon^{+}_{\mathrm{HOMO}}$	$\epsilon^{+}_{\mathrm{LUMO}}$	$\epsilon^{-}_{\mathrm{HOMO}}$	$\epsilon^{-}_{\mathrm{LUMO}}$	Δ_1	Δ_2
Fe_9O_6	−10.993	−10.780	−11.103	−10.953	0.040	0.323
Co_9O_6	−10.579	−10.113	−10.381	−10.370	0.209	0.268
Ni_9O_6	−9.448	−9.154	−9.316	−9.305	0.143	0.162

TABLE VI. Occupation numbers and moments of atomic orbitals in Fe_9O_6 clusters with C_{2v} symmetry, where the numbers in parentheses are moments (in μ_b), δq is the net charge, and the orbitals are $3d$, $4s$, $4p$ for the Fe atom, and $2s$, $2p$ for the O atom.

Atom	$3d$	$4s(2s)$	$4p(2p)$	δq	μ
Fe1	6.4272	0.5040	0.4545	+0.6143	
	(1.8661)	(0.0209)	(−0.0072)		1.8998
Fe2	6.3571	0.6172	0.3825	+0.6432	
	(1.7782)	(0.0661)	(0.0140)		1.8583
Fe3	6.2749	0.4071	1.6341	−0.3160	
	(2.6591)	(0.0199)	(0.2016)		2.8806
Fe4	6.2152	0.7478	0.3637	+0.6733	
	(1.6435)	(0.0619)	(0.0145)		1.7199
O1		1.9228	4.4359	−0.3587	
		(0.0009)	(−0.1185)		−0.1176
O2		1.9334	4.3113	−0.2446	
		(0.0050)	(−0.1492)		−0.1442

TABLE VII. Occupation numbers and moments of atomic orbitals in Co_9O_6 clusters with C_{2v} symmetry, where the numbers in parentheses are moments (in μ_b), δq is the net charge, and the orbitals are $3d$, $4s$, $4p$ for the Co atom, and $2s$, $2p$ for the O atom.

Atom	$3d$	$4s(2s)$	$4p(2p)$	δq	μ
Co1	7.5470	0.4545	0.4930	+0.5955	
	(0.9852)	(−0.0086)	(−0.0063)		0.8929
Co2	7.3580	0.6688	0.3549	+0.6183	
	(0.7187)	(−0.0090)	(−0.0035)		0.7062
Co3	7.3211	0.4607	1.5319	−0.3138	
	(1.3880)	(−0.0077)	(−0.0156)		1.3647
Co4	7.2956	0.5380	0.3705	+0.7959	
	(0.7775)	(−0.0131)	(0.0021)		0.7665
O1		1.9195	4.4384	−0.3580	
		(0.0035)	(−0.0856)		−0.050
O2		1.9190	4.3493	−0.2683	
		(0.0027)	(−0.1278)		−0.1251

shown in Fig. 3, and the skeleton composed of nine metal atoms also has C_{2v} symmetry, which is different from the structures of the pure transition-metal cluster M_9 (see Fig. 2), indicating that the structure transition in cluster can be caused by oxidation. For Fe_9O_6, Co_9O_6, and Ni_9O_6 clusters, the common geometric feature is that the O atoms are energetically more favorable to cap the triangle surfaces. The pair distribution functions for the C_{2v} structure are given in Fig. 4, and the bond lengths and bond angles are listed in Table II, where α_1, α_2, α_3, and α_4 are the bonding angles of $\angle$O1-M1-O1, $\angle$O1-M2-O1, $\angle$O1-M3-O2, and $\angle$O2-M4-O2, respectively.

Table III gives the data for the highest occupied molecular orbital (HOMO) and the lowest unoccupied molecular orbital (LUMO) for the C_{2v} structure, and Table IV lists the corresponding main orbital components. The HOMO's are mainly composed of O $2p$, M $4s$, and M $3d$ orbitals, while LUMO's are briefly attributed by O $2p$ and M $3d$ orbitals, but in the Co_9O_6 cluster, Co $3d$ orbitals have more weight.

To further confirm the stability of the C_{2v} structure, Table V lists the spin gaps, which are defined as $\Delta_1 = -(\epsilon^+_{\mathrm{HOMO}} - \epsilon^-_{\mathrm{LUMO}})$ and $\Delta_2 = -(\epsilon^-_{\mathrm{HOMO}} - \epsilon^+_{\mathrm{LUMO}})$ (+, spin up; −, spin down), corresponding to the energy required to move an infinitesimal amount of charge from the HOMO of one spin to the LUMO of the other. The positive values for both spin gaps can guarantee that the system is a stable magnetic and electronic state.[29,58] From Table V, we can see that these three oxide clusters with the C_{2v} structure are stable magnetically and electronically.

As for the charge transfer and magnetic properties, we have calculated the occupation numbers and moments of atomic orbitals of the M_9O_6 (M=Fe, Co, and Ni) cluster with C_{2v} symmetry, as listed in Tables VI, VII, and VIII, respectively. Comparing with the electronic configurations of $3d^{6(7,8)}4s^24p^0$ and $2s^22p^4$ for the isolated Fe, Co, Ni, and O atoms, O atoms are electron accepters with 0.2446 −0.4560 electrons transferred from $M1$, $M2$, and $M4$ atoms. Moreover, the $M3$ atom also gets electrons from $M1$, $M2$, and $M4$ atoms; In Fe_9O_6 and Co_9O_6 clusters, oxygen atoms are antiferromagnetically polarized, while ferromagnetically polarized in Ni_9O_6 cluster. This kind of ferromagnetism for O atoms has also been found in the system of oxygen ad-

TABLE VIII. Occupation numbers and moments of atomic orbitals in Ni_9O_6 clusters with C_{2v} symmetry, where the numbers in parentheses are moments (in μ_b), δq is the net charge, and the orbitals are $3d$, $4s$, $4p$ for the Ni atom, and $2s$, $2p$ for the O atom.

Atom	$3d$	$4s(2s)$	$4p(2p)$	δq	μ
Ni1	8.4162	0.5885	0.3748	+0.6205	
	(0.2932)	(0.0211)	(0.0017)		0.3160
Ni2	8.3932	0.6247	0.4243	+0.5579	
	(0.1415)	(0.0060)	(−0.0098)		0.1377
Ni3	8.3613	0.4252	1.3299	−0.1164	
	(0.0479)	(0.0068)	(−0.0019)		0.0528
Ni4	8.3409	0.6097	0.3693	+0.6801	
	(0.1969)	(0.0093)	(−0.0009)		0.2053
O1		1.8910	4.5650	−0.456 03	
		(0.0020)	(0.0905)		0.0925
O2		1.9029	4.4706	−0.3735	
		(0.0034)	(0.119 42)		0.1228

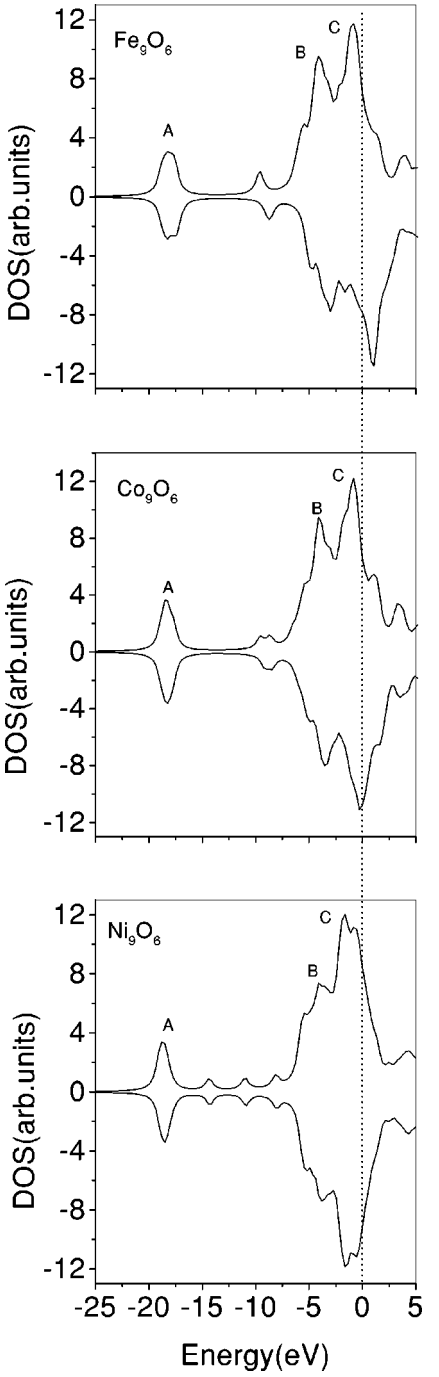

FIG. 5. Total densities of states for M_9O_6 clusters with C_{2v} symmetry.

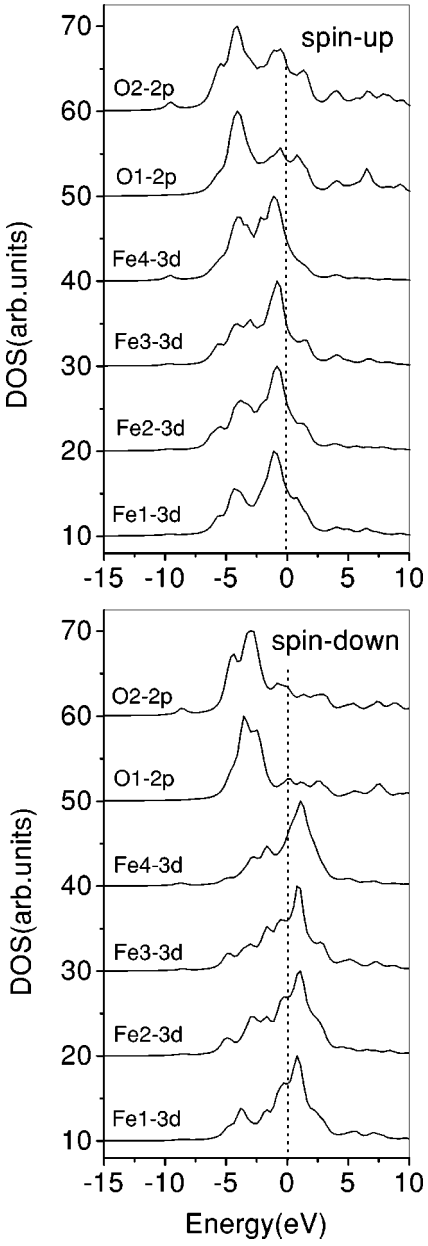

FIG. 6. Local densities of states (LDOS) for the Fe_9O_6 cluster with C_{2v} symmetry.

sorbed on the reconstructed Ni(110) surface.[59] The average local spin magnetic moments for the transition-metal atoms of Fe, Co, and Ni in these three clusters are 2.307, 1.050, and 0.147 μ_B, respectively, which are much reduced as compared to the values of 3.390, 2.310, and 0.940 μ_B in the bulk monoxides FeO, CoO, and NiO.[60] This is mainly due to the contraction of bond length in cluster as compared to the bulk values. A shorter bond length enables stronger hybridizations, and accordingly, the magnetic moments are reduced. In contrast to the antiferromagnetic arrangement of moments in the bulk monoxides FeO, CoO, and NiO, the moments of the transition-metal atoms in the clusters are ferromagnetically coupled. Due to the smaller size in the Fe_9O_6 cluster, the average magnetic moment of the Fe atom is enhanced, while the average binding energy per atom (5.489 eV) is reduced, as compared to the values of 2.061 μ_B and 5.648 eV in the $Fe_{13}O_8$ cluster,[25] which is also true for Co and Ni oxide clusters.

The magnetic properties above can be explained from the electronic structures. Figure 5 shows the total density of states (DOS) for these three clusters with C_{2v} symmetry, the dotted line is for Fermi level, which has been shifted to zero. There are three obvious peaks, labeled as *A*, *B*, and *C*, mainly contributed by O $2s$, O $2p$, and *M* $3d$ orbitals, respectively. The O $2s$ orbitals are much lower than *M* $3d$ orbitals, and the main interactions between *M* and O are O $2p$ and *M* $3d$ orbitals, where two competing factors exist. On going from Fe to Ni, the energy of the *d* level is reduced close to the *p* level of the O atom, so the $3d$-$2p$ interaction between *M* and O is increased. On the other hand, from Fe to Co to Ni, the *d*

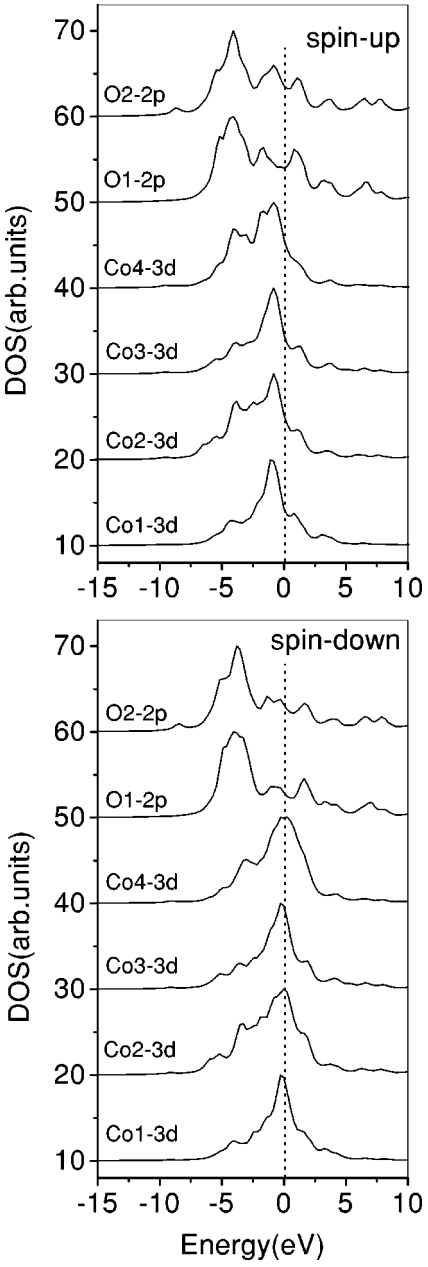

FIG. 7. Local densities of states (LDOS) for the Co_9O_6 cluster with C_{2v} symmetry.

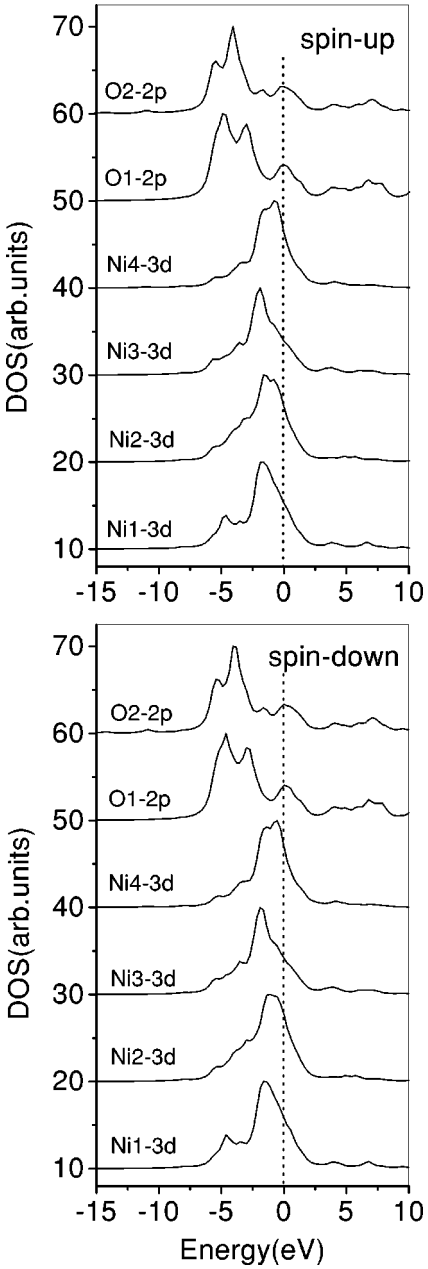

FIG. 8. Local densities of states (LDOS) for the Ni_9O_6 cluster with C_{2v} symmetry.

orbital is slightly contracted; accordingly the hybridization between O $2p$ and M $3d$ is reduced to some extent. The stability and magnetic behaviors are resulted from the compromise of these two competing factors. Compared with Fe_9O_6 and Co_9O_6, there are much more overlap and much stronger interactions between O $2p$ and Ni $3d$ orbitals in Ni_9O_6, which greatly reduces the magnetic moments of Ni atoms (the average moment is only $0.147\,\mu_B$). Figures 6–8 give the partial DOS of O $2p$ and M $3d$ of spin up and spin down.

As compared with Fe and Co, because the energy of $3d$ orbitals of the Ni atom is closer to the O $2p$ level, and due to exchange splittings, the spin-down $3d$ states have moved up in energy, the spin-up Ni $3d$ states have much stronger hybridization with O $2p$ states. As a result, O atoms are ferromagnetically polarized, but in Fe_9O_6 and Co_9O_6, the spin-down $3d$ states have stronger hybridizations with O $2p$ states, and thus O atoms are antiferromagnetically polarized.

In summary, by using a reactive laser vaporized cluster source, the magic oxide clusters M_9O_6 (M=Fe, Co, Ni) are found. From the first-principles calculations, it has been suggested that C_{2v} structure is the most stable among the five isomers considered. Oxidation changes the structures of the clusters. As compared to $M_{13}O_8$, due to the smaller size, the M_9O_6 cluster has an enhanced magnetic moment and reduced average binding energy.

ACKNOWLEDGMENTS

The authors would like to express their sincere thanks to Dr. G. Kresse and Dr. Y. Hashi for their kind help in our calculations, to Dr. V. Kumar for discussions, and to the

Materials Information Science Group of the Institute for Materials Research, Tohoku University, for their continuous support of the HITAC S-3800/380 supercomputing facility. This work is supported by a Grant-in-Aid for Scientific Research (08505004) from the Ministry of Education, Science, Culture and Sports of Japan, and from CREST (Core Research for Evolutional Science and Technology) of the Japan Science and Technology Corporation (JST).

[1] J. E. Campana, T. M. Barlak, R. J. Coton, J. J. DeCorpo, J. R. Wyatt, and B. I. Dunlap, Phys. Rev. Lett. **47**, 1046 (1981).
[2] O. Echt, K. Sattler, and E. Recknagel, Phys. Rev. Lett. **47**, 1121 (1981).
[3] For example, see the special issue in Science **217**, 10 (1996).
[4] P. Lievens, P. Thoen, and S. Bouckaert, J. Chem. Phys. **110**, 10 316 (1999).
[5] F. Finocchi and C. Noguera, Phys. Rev. B **57**, 14 646 (1998).
[6] F. Finocchi and C. Noguera, Phys. Rev. B **53**, 4989 (1996).
[7] N. Malinowski, H. Schabler, T. Bergmann, and T. P. Martin, Solid State Commun. **69**, 733 (1989).
[8] A. Nakajima, T. Sugioka, K. Hoshino, and K. Kaya, Chem. Phys. Lett. **189**, 455 (1992).
[9] T. Bergmann, H. Limberger, and T. P. Martin, Phys. Rev. Lett. **60**, 1767 (1988).
[10] T. P. Martin and T. Bergmann, J. Chem. Phys. **90**, 2848 (1989).
[11] T. P. Martin and B. Wassermann, J. Chem. Phys. **90**, 5108 (1989).
[12] W. A. Saunders, Phys. Rev. B **37**, 6583 (1988).
[13] S. Moukouri and C. Noguera, Z. Phys. D: At., Mol. Clusters **27**, 79 (1993).
[14] T. P. Martin and T. Bergmann, J. Chem. Phys. **90**, 6664 (1989).
[15] J. M. Recio and R. Pandey, Phys. Rev. A **47**, 2075 (1993).
[16] P. J. Ziemann and A. W. Castleman, Jr., J. Chem. Phys. **94**, 718 (1991).
[17] V. Boutou, M. A. Lebeault, A. R. Allouche, C. Bordas, F. Pauling, J. Viallon, and J. Chevaleyre, Phys. Rev. Lett. **80**, 2817 (1998).
[18] H. Wu, X. Li, X. B. Wang, C. F. Ding, and L. S. Wang, J. Chem. Phys. **109**, 449 (1999).
[19] T. Campell, R. K. Kalia, A. Nakano, and P. Vashishta, Phys. Rev. Lett. **82**, 4866 (1999).
[20] S. R. Desai, H. Wu, C. M. Rohlfing, and L. S. Wang, J. Chem. Phys. **106**, 1309 (1997).
[21] B. Kaiser, T. M. Bernhardt, M. Kinne, and K. Rademann, J. Chem. Phys. **110**, 1437 (1999).
[22] L. S. Wang, H. B. Wu, and S. R. Desai, Phys. Rev. Lett. **76**, 4853 (1996).
[23] L. S. Wang, J. W. Fan, and L. Lou, Surf. Rev. Lett. **3**, 695 (1996).
[24] H. B. Wu, S. R. Desai, and L. S. Wang, J. Am. Chem. Soc. **118**, 5296 (1996).
[25] Q. Wang, Q. Sun, M. Sakurai, J. Z. Yu, B. L. Gu, K. Sumiyama, and Y. Kawazoe, Phys. Rev. B **59**, 12 672 (1999).
[26] M. Sakurai, K. Sumiyama, Q. Sun, and Y. Kawazoe, J. Phys. Soc. Jpn. **68**, 3497 (1999).
[27] Q. Sun, Q. Wang, K. Parlinski, J. Z. Yu, Y. Hashi, X. G. Gong, and Y. Kawazoe, Phys. Rev. B **61**, 5781 (2000).
[28] S. K. Nayak and P. Jena, Phys. Rev. Lett. **81**, 2970 (1998).
[29] M. R. Pederson and S. N. Khanna, Phys. Rev. B **59**, R693 (1999).
[30] M. R. Pederson and S. N. Khanna, Phys. Rev. B **60**, 9566 (1999).
[31] M. R. Pederson and S. N. Khanna, Chem. Phys. Lett. **307**, 253 (1999).
[32] S. Y. Wang, L. J. Zou, X. G. Gong, Q. Q. Zheng, and H. Q. Lin, J. Appl. Phys. **83**, 7100 (1998).
[33] D. Arčon, J. Dolinšek, T. Apih, and R. Blinc, Phys. Rev. B **58**, R2941 (1998).
[34] R. B. Freas, B. I. Dunlap, B. A. Waite, and J. E. Campana, J. Chem. Phys. **86**, 1276 (1987).
[35] H. B. Wu and L. S. Wang, J. Chem. Phys. **107**, 16 (1997).
[36] M. Dolg, U. Wedig, H. Stoll, and H. Preuss, J. Chem. Phys. **86**, 2123 (1986).
[37] C. W. Bauschlicher, Jr. and P. Maitre, Theor. Chem. Acc. **90**, 189 (1995).
[38] M. Sakurai, K. Watanabe, K. Sumiyama, and K. Suzuki, J. Chem. Phys. **111**, 235 (1999).
[39] M. Sakurai, K. Watanabe, K. Sumiyama, and K. Suzuki, J. Phys. Soc. Jpn. **67**, 2571 (1998).
[40] M. Sakurai (unpublished).
[41] R. Car and M. Parrinello, Phys. Rev. Lett. **55**, 2471 (1985).
[42] M. C. Payne, M. P. Teter, D. C. Allan, T. A. Arias, and J. D. Joannopoulos, Rev. Mod. Phys. **64**, 1045 (1992).
[43] W. A. de Heer, Rev. Mod. Phys. **65**, 611 (1993).
[44] C. Massobrio, A. Pasquarello, and R. Car, Phys. Rev. Lett. **75**, 2104 (1995).
[45] D. Vanderbilt, Phys. Rev. B **41**, 7892 (1990).
[46] G. Kresse and J. Hafner, J. Phys.: Condens. Matter **6**, 8245 (1994).
[47] G. Kresse and J. Hafner, Phys. Rev. B **47**, 558 (1993); **49**, 14 251 (1994).
[48] G. Kresse and J. Furthmüller, Phys. Rev. B **54**, 11 169 (1996).
[49] Q. Sun, X. G. Gong, Q. Q. Zheng, D. Y. Sun, and G. H. Wang, Phys. Rev. B **54**, 10 896 (1996).
[50] D. E. Ellis and G. S. Painter, Phys. Rev. **2**, 2887 (1970).
[51] A. N. Andriotis and M. Menon, Phys. Rev. B **57**, 10 069 (1998).
[52] L. S. Wang, H. S. Cheng, and J. W. Fan, Chem. Phys. Lett. **236**, 57 (1995).
[53] M. S. Stave and A. E. DePristo, J. Chem. Phys. **97**, 3386 (1992).
[54] M. J. López and J. Jellinek, Phys. Rev. A **50**, 1445 (1994).
[55] S. K. Nayak, S. N. Khanna, B. K. Rao, and P. Jena, J. Phys. Chem. A **101**, 1072 (1997).
[56] G. M. Koretsky, K. P. Kerns, G. C. Nieman, M. B. Knickelbein, and S. J. Riley, J. Phys. Chem. A **103**, 1997 (1999).
[57] D. M. P. Mingos and D. J. Wales, *Introduction to Cluster Chemistry* (Prentice-Hall, Englewood Cliffs, NJ, 1990), p. 231.
[58] M. R. Pederson, F. Reuse, and S. N. Khanna, Phys. Rev. B **58**, 5632 (1998).
[59] R. Fournier and D. R. Salahub, Surf. Sci. **245**, 263 (1991).
[60] M. Takahashi and J. Igarashi, Phys. Rev. B **54**, 13 566 (1996).